2nd International Conference on the Material Point Method for Modelling Soil-Water-Structure Interaction

Anura3D
MPM Research Community

Paper number: mpm2019.23
www.anura3d.com
www.mpm2019.eu

Modelling large deflection of a poroelastic beam with an implicit iteratively coupled material point method

Hilde Aas Nøst[1,*], Gustav Grimstad[1]

[1]Department of Civil and Environmental Engineering, Norwegian University of Science and Technology, Trondheim, Norway

[*] E-mail: hilde.nost@ntnu.no

ABSTRACT

The existing approaches for coupled flow problems with material point method are using explicit time integration. This paper presents a material point method with implicit time integration for solving large deformation coupled flow-displacements problems. The method uses an iteratively coupled approach that splits the fully coupled system into two parts which can be solved by separate solvers. In this paper, the material point method solves the momentum equation, while the finite volume method solves the fluid mass equation. The method is used to model a coupled flow large deformation example of the bending of a poroelastic beam.

KEY WORDS: Material point method; large deformation; implicit time integration; soil-water interaction; saturated porous media.

INTRODUCTION

Several approaches for solving coupled flow-displacements problems with the material point method (MPM) have been developed. Examples include: The 1-point velocity formulations for saturated conditions (Jassim, Stolle and Vermeer, 2013) and unsaturated conditions (Yerro, Alonso and Pinyol, 2015); The 2-point formulations (Zhang *et al.*, 2008; Abe *et al.*, 2014; Bandara and Soga, 2015), where the water and solid phases have separate sets of particles; and the coupling of MPM with the finite difference method (Higo *et al.*, 2010). All of the above-mentioned approaches use explicit time integration.

Explicit time integration is suitable for high-velocity problems and problems where all stress waves are needed. However, implicit time integration is considered more accurate for slower types of coupled problems (Sheng and Sloan, 2003; Wang *et al.*, 2016). There exist several implicit time integration approaches with single-phase MPM (Guilkey and Weiss, 2003; Sulsky and Kaul, 2004; Love and Sulsky, 2006; Wang *et al.*, 2016). Although the quasi-static implicit MPM of Beuth (2012) tracked excess pore pressures, the method was undrained and did not consider the dissipation process. To the authors' knowledge, coupled analysis is not widely done together with implicit time integration in MPM. This paper aims to provide an approach for modelling of coupled flow-displacements problems with large deformations, that uses implicit time integration.

The approach of iterative coupling of the displacements and the flow has been in use for some time in the field of reservoir engineering (Fung, Buchanan and Wan, 1994; Settari and Mourits, 1998; Minkoff *et al.*, 2003; Kim, 2010). With iterative coupling, the displacements and flow can be solved by their own separate solver. One variable is kept constant while solving for the other, and then the updated variable is kept constant while the first is updated. This is done iteratively until convergence. The accuracy is equal to the traditional fully coupled approach (Settari and Mourits, 1998; Mikelić and Wheeler, 2013; Mikelić, Wang and Wheeler, 2014). The finite element method (FEM) as the mechanical solver has been coupled with the finite volume method (FVM) as the flow solver by for instance (Dean *et al.*, 2006; Phillips and Wheeler, 2007; Jha and Juanes, 2014). FEM and MPM share several properties, and therefore this coupling approach is feasible for MPM too. This paper will adapt the implicit iteratively coupled approach for MPM and FVM for saturated soils, and apply it on a

poroelastic beam.

FORMULATION OF THE ITERATIVELY COUPLED MATERIAL POINT METHOD

Governing equations

The iteratively coupled implicit MPM uses a quasi-static **u**-p formulation in this paper, with displacements **u** and pore pressures p as the primary variables. The first equation is the conservation of linear momentum for the mixture:

$$\boldsymbol{\nabla} \cdot \boldsymbol{\sigma}' + \boldsymbol{\nabla} p + \rho \mathbf{g} = \mathbf{0}, \tag{1}$$

where p is the pore pressure, $\boldsymbol{\sigma}'$ is the effective stress, **g** is the vector of gravitational acceleration, and ρ is the saturated density of the mixture defined by

$$\rho \; = \; n\rho_{\mathrm{w}} \; + \; (1 - n)\, \rho_{\mathrm{s}}, \tag{2}$$

where n is the porosity of soil, and ρ_{w} and ρ_{s} are the phase densities of water and soil grains, respectively.

The second equation is the conservation of fluid mass or storage equation:

$$\frac{n}{K_{\mathrm{w}}} \dot{p} - \dot{\varepsilon}_v \; - \boldsymbol{\nabla} \cdot \mathbf{q} \; = \; 0, \tag{3}$$

where K_{w} is the fluid bulk modulus, $\dot{\varepsilon}_v = \boldsymbol{\nabla} \cdot \dot{\mathbf{u}}$ is the volumetric strain rate,and **q** is the Darcy velocity given by Darcy's law:

$$\mathbf{q} \; = \; - \frac{k}{\rho_{\mathrm{w}} g} (\boldsymbol{\nabla} p \; - \; \rho_{\mathrm{w}} \mathbf{g}), \tag{4}$$

where k is the hydraulic conductivity.

Any constitutive model can be used to describe the relation between effective stress and strain. An isotropiclinear elastic material is used in this paper.

The fully coupled implicit system of equations

The linear momentum conservation equation (1) is discretised as the original MPM. The deforming body is discretised as material points. The equation is multiplied by a test function and integrated over the domain. The mass matrix is diagonally lumped, and the standard linear shape functions are used. The storage equation (3) is discretised with piecewise constant test and shape functions, which is equivalent to FVM. Then semi-discretised system of equations is as follows:

$$\begin{bmatrix} \mathbf{0} & \mathbf{0} \\ \mathbf{Q}_2 & \mathbf{C} \end{bmatrix} \begin{bmatrix} \dot{\mathbf{u}} \\ \dot{\mathbf{p}} \end{bmatrix} + \begin{bmatrix} -\mathbf{K} & \mathbf{Q}_1 \\ \mathbf{0} & \mathbf{T} \end{bmatrix} \begin{bmatrix} \mathbf{u} \\ \mathbf{p} \end{bmatrix} = \begin{bmatrix} \mathbf{F}_{\mathrm{ext}} \\ \mathbf{F}_{\mathrm{ext,w}} \end{bmatrix}, \tag{5}$$

where $\mathbf{Q}_2 = \mathbf{Q}_1^{\mathrm{T}}$ are the coupling matrices, **C** is the fluid compressibility matrix, and **T** is the transmissibility matrix.

The simple backwards Euler scheme is applied as the time integration method. The time derivatives of the variables are approximated by $\dot{\mathbf{p}} \approx (\mathbf{p}^{n+1} - \mathbf{p}^n)/\Delta t$and $\dot{\mathbf{u}} \approx (\mathbf{u}^{n+1} - \mathbf{u}^n)/\Delta t$, where superscripts n and $n+1$ denote values at times t and $t + \Delta t$, respectively. After multiplying the second row of the fully discretised Equation (5) with Δt and moving all known quantities to the right hand side, gives the fully coupled implicit system of equations as

$$\begin{bmatrix} -\mathbf{K} & \mathbf{Q}_1 \\ \mathbf{Q}_2 & \mathbf{C} - \Delta \mathrm{t}\, \mathbf{T} \end{bmatrix} \begin{bmatrix} \mathbf{u}^{n+1} \\ \mathbf{p}^{n+1} \end{bmatrix} = \begin{bmatrix} \mathbf{F}_{\mathrm{ext}} \\ \Delta t \mathbf{F}_{\mathrm{ext,w}} + \mathbf{C}\mathbf{p}^n \end{bmatrix}. \tag{6}$$

The grid is reset at the beginning of each time step n. Consequently, the displacements $\mathbf{u}^n = \mathbf{0}$.

The iteratively coupled implicit system of equations

White, Castelletto and Tchelepi (2016) showed that the fixed-stress operator split as presented by Kim, Tchelepi and Juanes (2011) is equal to applying an upper triangular block preconditioner such as

$$\mathbf{P} = \begin{bmatrix} -\mathbf{K} & \mathbf{Q}_1 \\ \mathbf{0} & \tilde{\mathbf{S}}_A \end{bmatrix} \tag{7}$$

to the fully coupled system in Equation (6). This results in a triangular preconditioned Richardson iteration system

$$\begin{bmatrix} -\mathbf{K} & \mathbf{Q}_1 \\ \mathbf{0} & \tilde{\mathbf{S}}_A \end{bmatrix} \begin{bmatrix} \mathbf{u}^{k+1} \\ \mathbf{p}^{k+1} \end{bmatrix} = \begin{bmatrix} \mathbf{0} & \mathbf{0} \\ -\mathbf{Q}_2 & \frac{1}{K_{\mathrm{w}}} \mathbf{M}_{\mathrm{p}} \end{bmatrix} \begin{bmatrix} \mathbf{u}^{k} \\ \mathbf{p}^{k} \end{bmatrix} + \begin{bmatrix} \mathbf{F}_{\mathrm{ext}} \\ \Delta t \mathbf{F}_{\mathrm{ext,w}} + \mathbf{C}\mathbf{p}^n \end{bmatrix}, \tag{8}$$

where superscripts k and $k+1$ indicate the iteration number at time step $n+1$, and the Schur complement approximation is

$$\tilde{\mathbf{S}}_A = \mathbf{C} - \boldsymbol{\Delta} t\, \mathbf{T} + \frac{1}{K_{\mathrm{w}}} \mathbf{M}_p \tag{9}$$

where $\mathbf{M}_p$ is a diagonal matrix with the cell volume on its diagonal. The advantage of the system in Equation (8) to the fully implicit system in Equation (6) is that it can be easily solved by first solving for pore pressures and then the displacements without the need to invert the large block coefficient matrix.

The Schur complement $\tilde{\mathbf{S}}_A$ is a sparse symmetric positive-definite matrix. The conjugate gradient method can therefore be applied when solving the second row of Equation (8).

LARGE DEFLECTION OF A POROELASTIC BEAM

A poroelastic beam subject to a distributed load is modelled to verify that the proposed method can model coupled flow large deformation problems. Two-way coupled flow and displacements is when the displacements affect the pore pressure and that the pore pressure affects the displacements. Pore pressures should be generated in the beam due to the bending moment generated by the applied load. In addition, the beam deflection should increase further as the initial pore pressures dissipate.

Model setup

A cantilever poroelastic beam is modelled. The length of the beam $L = 1$ m in the x-direction, with height $h = 0.3$ m in the y-direction, and depth $d = 0.1$ m in the z-direction. The end at $x = 0$ m is fixed and the end at $x = L$ is free to bend and move. The flow boundary conditions are permeable at $x = 0$ m and $x = L$, while the remaining sides of the beam are impermeable.

The material is a fully-saturated, isotropic linear elastic material. The stiffness moduli are $K = 3{,}333\,333$ MPa and $G = 5$ MPa. The poroelastic properties are: hydraulic conductivity $k = 10^{-4}\mathrm{m/s}$, bulk modulus of water $K_{\mathrm{w}} = 2.2$ GPa, and initial porosity $n = 0.4$. The water density is $\rho_{\mathrm{w}} = 1\,000\ \mathrm{kg/m^3}$ and the saturated density $\rho = 2\,000\ \mathrm{kg/m^3}$.

The applied distributed load is $q = 54$ kPa. The load q is applied along the top side of the beam, starting from position $x = 0.05$ m running until the free end at $x = L$. The load q is applied as fast as possible, which in this case is at $t = 0.06$ s. The size of the time step was chosen to be $\Delta t = 2 \cdot 10^{-2}$s to minimise initial oscillations in pore pressure response.

The computational grid is defined with $\Delta y = \Delta x =$ 0.015 m and only 1 cell in the out-of-plane z-direction. The total grid size of $y =$ 1.2 m, $x =$ 1.5 m and $z =$ 0.1 mgives a total of 8000 cells, of which 1407 cells contain the beam material at initialisation. In each cell $2 \times 2 \times 1$ particles are initialised in x-, y-, and z-direction, respectively. This gives 4 particles per cell. Not all cells were fully filled with particles at creation. A total of 5320 particles were created in the domain.

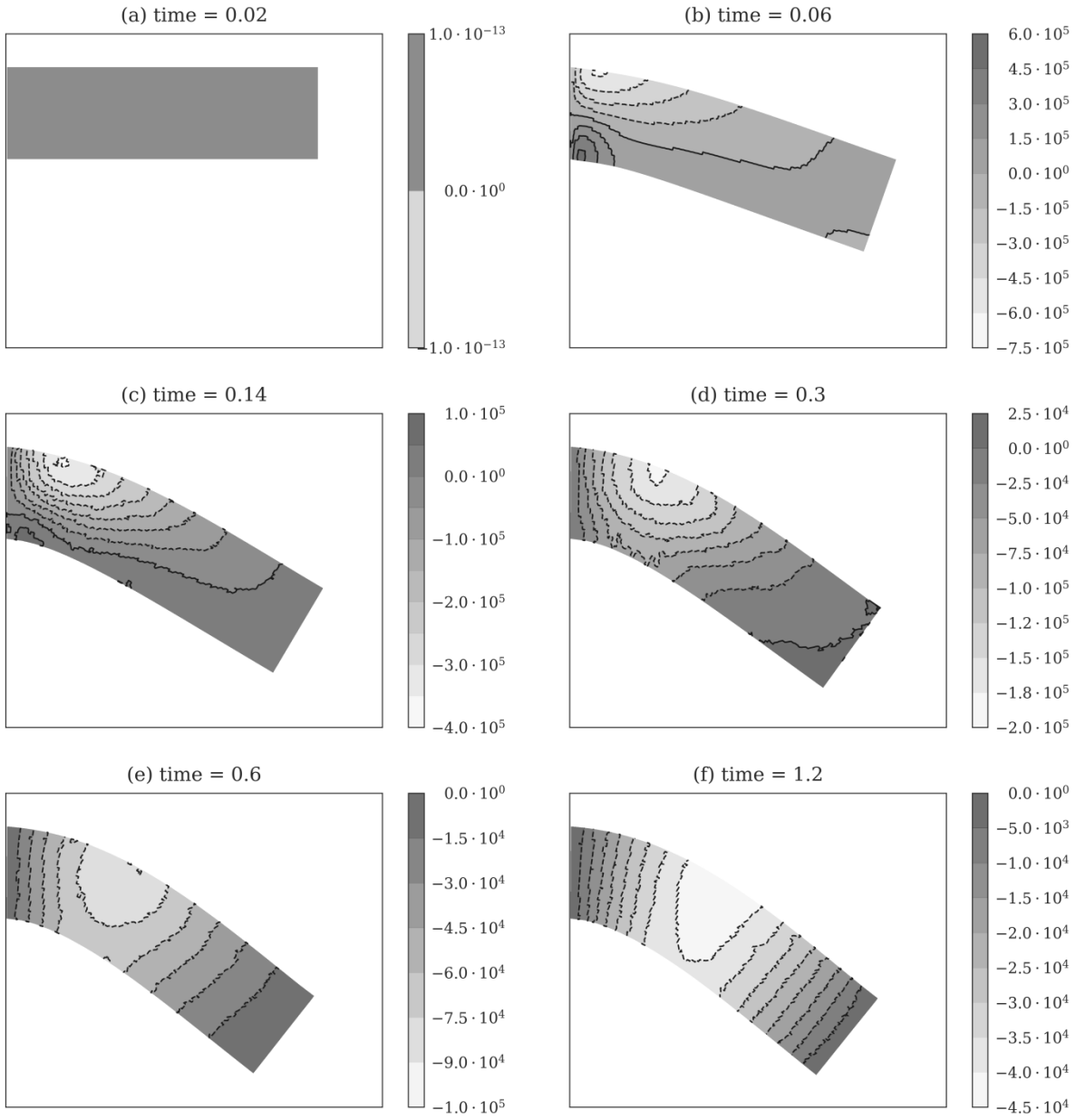

Figure 1 Material point pore pressure distribution in the poroelastic beam subject to a distributed load of q=54 kPa. Pore pressures are in Pascal, with suction negative. Time is in seconds.

Results and discussion

Figure 1 shows the pore pressure generation and dissipation in time in the poroelastic beam. First, notice from Figure 1 (b) that the bending moment generates pore pressures in the poroelastic beam. There is suction in the

upper part of the beam that experiences stretching, and there is pressure in the lower part of the beam that experiences compression, see Figures 1 (b) to (c). This is physically viable. Figures 1(c) to (f) show the pore pressure dissipation process. Figure 1 shows that the proposed method generates pore pressures based on displacements and dissipates the pore pressures while maintaining the largely deformed state. The pore pressures are dissipated in both the axial and the transverse directions. Furthermore, in Figure 1(f) the boundary conditions give a pore pressure distribution similar to the pore pressure distribution of the one-dimensional two-way drainage consolidation problem. However, the pore pressures in the beam at the end of the simulation are in suction because the distributed load is applied in the negative Cartesian y-direction which causes the beam to stretch. Overall, the physics of the simulations seems correct.

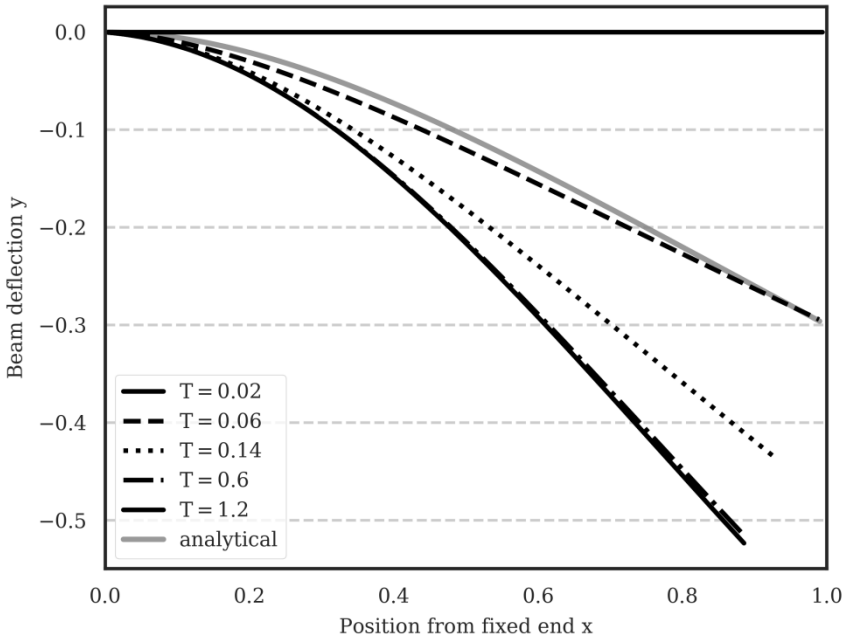

Figure 2 Deflection curves of the poroelastic beam at various simulation times. Time is in seconds, length is in metres.

The beam deflection curves at various time intervals are shown in Figure 2. In theory, the initial deflection of the beam should correspond to the linear elastic quasi-static solution of beam bending. However, as seen in Figure2, there is a small deviation from the analytical solution, though only in the curvature. This may be due to Euler-Bernoulli beam theory which disregards shear deformations. After the initial deflection, there is an additional increase in deflection plotted in Figure 2. The load has already been applied and a displacement has already resulted from that load, as discussed in the previous paragraph. Therefore, the additional deflection stems from the pore pressure dissipation. The beam will give a softer response as pore pressures decrease. From Figure 2, there is very little change in deflection between t = 0.6 s and t = 1.2 s. However, Figure 1 e) shows the pore pressure distribution in the beam at $t = 0.6$ s, but all pore pressures have not dissipated yet. Consequently, the maximum deflection is obtained when the pore pressures are approximately equal along the beam cross-section. Overall, Figure 2 shows that the pore pressure cross-sectional distribution influences the displacement response.

CONCLUSION

An iteratively coupled implicit MPM-FVM has briefly been presented. Then, the proposed method has been applied to a poroelastic beam subject to a distributed load that gives a large deflection. The results indicate that the proposed method is able to model large deformations that also include cell-crossing of particles, and model two-way coupled flow and displacements.

REFERENCES

Abe, K. *et al.* (2014) 'Material Point Method for Coupled Hydromechanical Problems', *Journal of Geotechnical and*

Geoenvironmental Engineering. American Society of Civil Engineers, 140(3), p. 04013033. doi: 10.1061/(ASCE)GT.1943-5606.0001011.
Bandara, S. and Soga, K. (2015) 'Coupling of soil deformation and pore fluid flow using material point method', *Computers and Geotechnics*, 63, pp. 199–214. doi: 10.1016/j.compgeo.2014.09.009.
Beuth, L. (2012) *Formulation and Application of a Quasi-Static Material Point Method*. Universität Stuttgart.
Dean, R. H. *et al.* (2006) 'A Comparison of Techniques for Coupling Porous Flow and Geomechanics', *SPE Journal*, 11(01), pp. 132–140.
Fung, L. S.-K., Buchanan, L. and Wan, R. G. (1994) 'Coupled Geomechanical-thermal Simulation for Deforming Heavy-oil Reservoirs', *Journal of Canadian Petroleum Technology*, 33(4), pp. 22–28.
Guilkey, J. E. and Weiss, J. A. (2003) 'Implicit time integration for the material point method: Quantitative and algorithmic comparisons with the finite element method', *International Journal for Numerical Methods in Engineering*. John Wiley & Sons, Ltd., 57(9), pp. 1323–1338. doi: 10.1002/nme.729.
Higo, Y. *et al.* (2010) 'A Coupled MPM-FDM Analysis Method for Multi-Phase Elasto-Plastic Soils', *Soils and Foundations*, 50(4), pp. 515–532. doi: 10.3208/sandf.50.515.
Jassim, I., Stolle, D. and Vermeer, P. (2013) 'Two-phase dynamic analysis by material point method', *International Journal for Numerical and Analytical Methods in Geomechanics*, 37(15), pp. 2502–2522. doi: 10.1002/nag.2146.
Jha, B. and Juanes, R. (2014) 'Coupled multiphase flow and poromechanics: A computational model of pore pressure effects on fault slip and earthquake triggering', *Water Resources Research*, 50, pp. 3776–3808. doi: 10.1002/2013WR015175.
Kim, J. (2010) *Sequential Methods for Coupled Geomechanics and Multiphase Flow*. Stanford.
Kim, J., Tchelepi, H. A. and Juanes, R. (2011) 'Stability and convergence of sequential methods for coupled flow and geomechanics: Fixed-stress and fixed-strain splits', *Computer Methods in Applied Mechanics and Engineering*. North-Holland, 200(13–16), pp. 1591–1606. doi: 10.1016/J.CMA.2010.12.022.
Love, E. and Sulsky, D. L. (2006) 'An unconditionally stable, energy–momentum consistent implementation of the material-point method', *Computer methods in applied mechanics and engineering*, 195, pp. 3903–3925. doi: 10.1016/j.cma.2005.06.027.
Mikelić, A., Wang, B. and Wheeler, M. F. (2014) 'Numerical convergence study of iterative coupling for coupled flow and geomechanics', *Computational Geosciences*, 18(3–4), pp. 325–341. doi: 10.1007/s10596-013-9393-8.
Mikelić, A. and Wheeler, M. F. (2013) 'Convergence of iterative coupling for coupled flow and geomechanics', *Computational Geosciences*. Springer Netherlands, 17(3), pp. 455–461. doi: 10.1007/s10596-012-9318-y.
Minkoff, S. E. *et al.* (2003) 'Coupled fluid flow and geomechanical deformation modeling', *Journal of Petroleum Science and Engineering*. Elsevier, 38(1–2), pp. 37–56. doi: 10.1016/S0920-4105(03)00021-4.
Phillips, P. J. and Wheeler, M. F. (2007) 'A coupling of mixed and continuous Galerkin finite element methods for poroelasticity I: the continuous in time case', *Computational Geosciences*. Kluwer Academic Publishers, 11(2), pp. 131–144. doi: 10.1007/s10596-007-9045-y.
Settari, A. and Mourits, F. M. (1998) 'A Coupled Reservoir and Geomechanical Simulation System', *SPE Journal*, 3(03), pp. 219–226.
Sheng, D. and Sloan, S. W. (2003) 'Time stepping schemes for coupled displacement and pore pressure analysis', *Computational Mechanics*. Springer-Verlag, 31(1–2), pp. 122–134. doi: 10.1007/s00466-002-0399-7.
Sulsky, D. and Kaul, A. (2004) 'Implicit dynamics in the material-point method', *Computer Methods in Applied Mechanics and Engineering*, 193, pp. 1137–1170. doi: 10.1016/j.cma.2003.12.011.
Wang, B. *et al.* (2016) 'Development of an implicit material point method for geotechnical applications', *Computers and Geotechnics*, 71, pp. 159–167. doi: 10.1016/j.compgeo.2015.08.008.
White, J. A., Castelletto, N. and Tchelepi, H. A. (2016) 'Block-partitioned solvers for coupled poromechanics: A unified framework', *Computer Methods in Applied Mechanics and Engineering*. North-Holland, 303, pp. 55–74. doi: 10.1016/j.jns.2003.09.014.
Yerro, A., Alonso, E. E. and Pinyol, N. M. (2015) 'The material point method for unsaturated soils', *Géotechnique*, 65(3), pp. 201–217. doi: 10.1680/geot.14.P.163.
Zhang, D. Z. *et al.*(2008) 'Material point method applied to multiphase flows', *Journal of Computational Physics*. Academic Press, 227(6), pp. 3159–3173. doi: 10.1016/j.jcp.2007.11.021.